Fabrication of Sol−Gel Materials with Anisotropic Physical Properties by Photo-Cross-Linking

C. Wingfield,[†] A. Baski,[†] M. F. Bertino,*[,†] N. Leventis,[‡] D. P. Mohite,[‡] and H. Lu[§]

Department of Physics, Virginia Commonwealth University, Richmond, Virginia 23284, Department of Chemistry, Missouri University of Science and Technology, Rolla, Missouri 65409, and Department of Mechanical and Aerospace Engineering, 218 Engineering North, Oklahoma State University, Stillwater, Oklahoma 74078

Received December 15, 2008. Revised Manuscript Received March 15, 2009

A method to vary locally the physical properties of a porous material is presented. A wet gel is first prepared following conventional sol−gel techniques. The pore walls are derivatized by adding to the gelling solution a silane carrying a polymerizable moiety such as trimethoxysilylpropyl. The solvent of the wet gel monolith is then exchanged with a solution of a monomer such as styrene and a photoinitiator such as 2,2′-azobis-isobutyronitrile. Illumination with ultraviolet light initiates polymerization which in turn engages the moiety dangling from the pore surfaces. Supercritically dried monoliths were characterized with techniques such as field-emission scanning electron microscopy (SEM), methylmethacrylate atomic force microscopy (AFM), Fourier transform infrared (FT-IR) spectroscopy, and Brunauer−Emmett−Teller surface area measurements. These structural characterization techniques showed that the silica nanoparticles making up the backbone of the monoliths were cross-linked by a polymer conformal coating. Mechanical characterization was carried out with nanoindentation and the three-point flexural method and showed that the properties of uniformly photo-cross-linked monoliths could be varied by varying exposure time. So, for example, the monolith density could be varied between about 0.21 and 0.97 $g \cdot cm^{-3}$, the porosity between 6 and 87%, and Young's modulus between 9 and about 1800 MPa. Overall, the characterization techniques show that photo-cross-linked monoliths have physical and mechanical properties comparable and often superior to those of monoliths obtained by thermally initiated cross-linking (see, for example, Leventis, N.; Sotiriou-Leventis, C.; Zhang, G.; Rawashdeh, A.-M. M. *Nano Lett.* **2002**, *2*, 957−960). More importantly photo-cross-linking allows fabrication of monoliths with anisotropic physical properties. We demonstrate the modulation capabilities of our method by producing transparent and opaque regions within the same monolith and by producing multifunctional two- and three-dimensional patterns.

1. Introduction

Sol−gel materials are currently being considered as building blocks for a wide variety of devices such as photonic crystals, thermal insulators, space dust and radiation collectors, low dielectric constant materials, and microfluidics components.[1] Methods have been developed to tailor the physical properties of sol−gel materials to the needs of a certain application. For example, porosity and pore size distribution can be controlled by forming micelles in a sol; [2−4] gels can be made hydrophobic by derivatizing the pore walls with hydrophobic moieties;[5] superhydrophilicity can be attained by ultraviolet irradiation; [6,7] mechanical strength can be increased by cross-linking the oxide nanoparticles that make up the gel;[1,8,9] and optical properties can be controlled by adding chromophores and nanoparticles to control the index of refraction, absorption, and luminescence.[10−12]

To date, most of the work has focused on the fabrication of thin films and/or monoliths whose properties have been modified uniformly throughout the volume. Sol−gel materials with spatially modulated properties have been reported comparatively seldom, and the research has been mostly limited to thin films. Modulations are most frequently obtained by etching; however, holographic techniques have also been reported.[13] For the NASA stardust project, density

* Corresponding author. E-mail: mfbertino@vcu.edu.
[†] Virginia Commonwealth University.
[‡] Missouri University of Science and Technology.
[§] Oklahoma State University.

(1) For a recent review on the synthesis and applications of aerogels, see: Pierre, A. C.; Pajonk, G. M. *Chem. Rev.* **2002**, *102*, 4243.
(2) Zhao, D.; Feng, J.; Huo, Q.; Melosh, N.; Fredrickson, G. H.; Chmelka, B.; Stucky, G. D. *Science* **1998**, *279*, 548.
(3) Amatani, T.; Nakanishi, K.; Hirao, K.; Kodaira, T. *Chem. Mater.* **2005**, *17*, 114.
(4) Heckman, B.; Martin, L.; Bertino, M. F.; Leventis, N.; Tokuhiro, A. T. *Sep. Sci. Technol.* **2008**, *43*, 1474.
(5) Brandhuber, D.; Peterlik, H.; Husing, N. *J. Mater. Chem.* **2005**, *15*, 3896.
(6) Langlet, M.; Permpoon, S.; Riassetto, D.; Berthome, G.; Pernot, E.; Joud, J. C. *J. Photochem. Photobiol., A* **2006**, *181*, 203.
(7) Bertino, M. F.; Smarsly, B.; Stocco, A.; Stark, A. *Adv. Funct. Mater.* **2009**, *19*, 1.
(8) (a) Leventis, N. *Acc. Chem. Res.* **2007**, *40*, 874. (b) Meador, M. A. B.; Capadona, L. A.; MacCorkle, L.; Papadopoulos, D. S.; Leventis, N. *Chem. Mater.* **2007**, *19*, 2247.
(9) Leventis, N.; Sotiriou-Leventis, C.; Zhang, G.; Rawashdeh, A.-M. M. *Nano Lett.* **2002**, *2*, 957.
(10) Wu, P.-W.; Cheng, W.; Martini, I. B.; Dunn, B.; Schwartz, B. J.; Yablonovitch, E. *Adv. Mater.* **2000**, *12*, 1438.
(11) Bertino, M. F.; Gadipalli, R. R.; Story, J. G.; Williams, C. G.; Zhang, Z.; Sotiriou-Leventis, C.; Tokuhiro, A. T.; Guha, S.; Leventis, N. *Appl. Phys. Lett.* **2004**, *85*, 6007.
(12) Bertino, M. F.; Gadipalli, R. R.; Martin, L. A.; Rich, L. E.; Yamilov, A.; Heckman, B. R.; Leventis, N.; Guha, S.; Katsoudas, J.; Divan, R.; Mancini, D. C. *Nanotechnology* **2007**, *18*, 315603.

10.1021/cm803374b CCC: $40.75
Published on Web 04/27/2009

gradients were introduced by depositing layers with decreasing sol concentrations.[14] Modulations within bulk monoliths have been reported by the Dunn group,[10] which produced three-dimensional Ag patterns by multiphoton reduction of Ag^+, and by our group which has produced metal and quantum dot patterns.[11,12,14−16] These bulk patterning techniques, however, have limitations. Nanoparticles grown inside the pores affect the optical properties but not, for example, the mechanical properties. In addition, nanoparticles may clog the pores and limit diffusion of fluids and analytes through the monoliths.[4]

Here, we introduce a method that allows fabrication of spatially anisotropic monoliths. In our method, a suitable olefin such as methacrylate or vinyl is first attached to the pore walls; the gelation solvent is then exchanged with a solution of a monomer and a photoinitiator. In exposed regions the monomer reacts with the moiety attached to the walls and cross-links the oxide nanoparticles making up the gels. Our group has shown that cross-linking by thermal activation yields lightweight sol−gel materials with high mechanical strength.[17] Photo-cross-linking yields monoliths with features comparable or superior to those of cross-linked monoliths reported to date. Most importantly, photo-cross-linking allows spatial modulation of the physical properties of the monoliths. By choosing an appropriate monomer it is possible to vary within the same monolith mechanical modulus, porosity, hydrophobicity, optical absorption and luminescence. The character of the patterns can be also varied by varying the wavelength of the incident light. Surface patterns are generated by using a wavelength that does not penetrate deeply into materials (e.g., 266 nm); three-dimensional patterns that penetrate several millimeters inside the monoliths are produced by using ultraviolet light with longer wavelengths.

2. Experimental Section

Materials. Tetramethylorthosilicate (TMOS), vinyltrimethoxysilane (VTMS), trimethoxysilylpropyl methylmethacrylate (MTMS), styrene, 9-vinylanthracene, 2,2′-azobis-isobutyronitrile (AIBN), ammonium hydroxide, and solvents (methanol, acetonitrile, and acetone) were all of ACS reagent grade and were used as received from Aldrich.

Preparation of Monoliths. Porous monoliths were generated following published procedures or slight modifications thereof.[18] Native silica gels were generated by dissolving 3.89 mL of TMOS in 4.5 mL of methanol. To this solution, another solution consisting of 4.5 mL of methanol, 1.5 mL of H_2O, and 40 μL of NH_4OH was added. After a brief period of vigorous agitation the solution was poured into molds and a gel was formed within a few hours. The gels were extruded from the molds, and the gelation byproducts were removed by repeated washings in methanol or by Soxhlet extraction. Gels prepared following this procedure had pore walls terminated with −OH groups and were employed mostly for control experiments. To obtain cross-linked monoliths, the pore walls were derivatized with a suitable olefin such as a methacrylate (MTMS) or vinyl (VTMS) group. This derivatization was obtained by replacing between 5 and 25% (v/v) of TMOS with MMTS (respectively, VTMS) in the parent solution.[19,20] In the following, monoliths that were not derivatized will be indicated as "native"; monoliths carrying olefins on the pore walls will be indicated as "derivatized".

Exposure. For photo-cross-linking the solvent of wet gels was exchanged with a solution of AIBN (typically about 0.1% w/w) in styrene. Prior to photo-cross-linking, the polymerization inhibitor was removed by passing the as-received styrene monomer on an alumina column. To prevent polymerization from starting before illumination, samples were kept refrigerated and in the dark while solvent exchange was being carried out. Shortly before exposure nitrogen was repeatedly bubbled through the bathing solution to remove oxygen. This deaeration procedure was extremely important, since oxygen-saturated samples were considerably weaker and had up to twice the porosity and smaller density than deaerated samples. Luminescent patterns were generated by exchanging the solvent of a gel with an acetonitrile solution containing 1% (w/w) of 9-vinylanthracene and 0.1% (w/w) of AIBN. Patterns were generated by photodissociating AIBN. To create uniformly cross-linked monoliths samples were exposed to a commercial 15 W black light or to a 30 mW He−Cd laser (325 nm) expanded by a divergent lens. To create surface patterns, a 175 mW continuous wave (CW) laser (Coherent MBD-266) emitting at a wavelength of 266 nm was employed. The 266 nm wavelength was strongly absorbed by both the matrix and the organics, resulting in patterns that did not penetrate more than a few micrometers. To create three-dimensional patterns the third harmonic (354 nm) of a pulsed yittrium aluminum garnet (Nd:YAG) laser (EKSPLA 312 G) was employed. Pulses had a duration of 150 ps and they were focused inside the bulk of monoliths by a lens with a focal length of 100 mm or by a long-working distance microscope objective. The mean pulse energy was kept below about 10 mJ to prevent damaging the matrix. Features were obtained with a size below about 30 μm. Exposure times were between 5 and 10 min when a laser was employed and up to 48 h for exposure with a black light. After exposure, monoliths were washed repeatedly with acetonitrile or toluene to remove unreacted precursors and polystyrene that was attached to the walls.

Characterization. Monoliths were characterized with standard techniques such as field-emission scanning electron microscopy (SEM), atomic force microscopy (AFM), and Fourier transform infrared (FT-IR) spectroscopy. Supercritical fluid (CO_2) drying was conducted using an autoclave (SPI-DRY Jumbo Supercritical Point Drier, SPI Supplies, Inc., West Chester, PA). Bulk densities (ρ_b) were calculated from the weight and the physical dimensions of the samples. Skeletal densities (ρ_s) were determined using helium pycnometry with a Micromeritics Accu Pyc II 1340 instrument. Porosities were determined from ρ_b and ρ_s. Mesoporous surface areas (σ) and pore size distributions were measured by nitrogen adsorption/desorption porosimetry using a Quantachrome Autosorb-1 Surface Area/Pore Distribution analyzer. Samples for surface area and skeletal density determination were outgassed for 24 h at 80 °C under vacuum before analysis. A nanoindentation

(13) Muir, A. C.; Mailis, S.; Eason, R. W. *J. Appl. Phys.* **2007**, *101*, 104916.
(14) Jones, S. M. *J. Sol-Gel Sci. Technol.* **2007**, *44*, 255.
(15) Gadipalli, R. R.; Martin, L. A.; Heckman, B.; Story, J. G.; Bertino, M. F.; Leventis, N.; Fraundorf, P.; Guha, S. *J. Sol-Gel Sci. Technol.* **2006**, *39*, 299.
(16) Gadipalli, R. R.; Martin, L. A.; Heckman, B.; Story, J. G.; Bertino, M. F.; Leventis, N.; Fraundorf, P.; Guha, S. *J. Sol-Gel Sci. Technol.* **2006**, *40*, 101.
(17) Bertino, M. F.; Hund, J. F.; Sosa, J.; Zhang, G.; Sotiriou-Leventis, C.; Leventis, N.; Tokuhiro, A. T.; Terry, J. *J. Sol-Gel Sci. Technol.* **2004**, *30*, 43.
(18) For a recent review on cross-linking of sol-gel materials, see: Leventis, N. *Acc. Chem. Res.* **2007**, *40*, 874.
(19) Hund, J. F.; Bertino, M. F.; Zhang, G.; Sotiriou-Leventis, C.; Leventis, N.; Tokuhiro, A. T.; Farmer, J. *J. Phys. Chem. B* **2003**, *107*, 465.
(20) Smarsly, B.; Garnweitner, G.; Assink, R.; Brinker, C. J. *Prog. Org. Coat.* **2003**, *47*, 393.

Scheme 1. Photo-Cross-Linking Mechanism of Skeletal Vinyl-Modified Silica Nanoparticles with Polystyrene

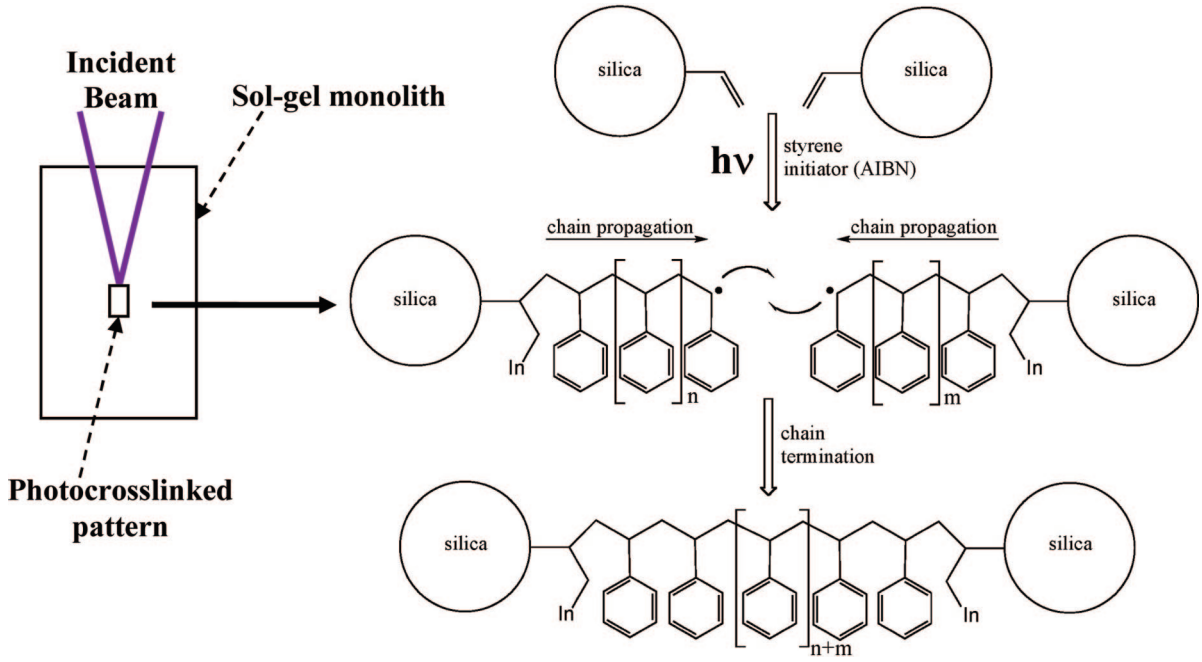

test was conducted on an MTS nanoindenter XP system equipped with a diamond spherical indenter tip with 10 μm radius, where 6 to 10 tests were conducted on each sample. All nanoindentations were conducted under constant loading rate history. Young's modulus and hardness of the samples can be calculated from nanoindentation measurements following the procedure described in refs 25 and 26.

3. Results and Discussion

In our photopolymerization scheme, the silica nanoparticles in illuminated regions are cross-linked as shown in Scheme 1. The method is simple and it can be adapted to a wide variety of surface chemistries and polymers. In Figure 1 we show luminescent patterns that were produced by exchanging the gelation solvent with a polymerizable luminescent moiety such as 9-vinylanthracene. Two- and three-dimensional patterns were fabricated by varying the type of laser and the illumination conditions. Surface patterns are shown in Figure 1a, and they were obtained by masking a continuous-wave laser emitting at a wavelength of 266 nm. The high absorbance of the matrix and of the organics in this spectral region confined the pattern to the monolith surface. Three-dimensional patterns were obtained by using ultraviolet light with longer wavelength such as the third harmonic (355 nm) of a pulsed Nd:YAG laser. Patterns extending deep inside monoliths were created by focusing the incident beam with a long (100 mm) focal length lens as shown in Figure 1b. A higher spatial resolution (up to about 20 μm) was obtained by focusing the light with a long working distance microscope objective as shown in Figure 1c. The light was focused about 1 mm below the surface, and the sample was moved in front of the beam with a motorized translation stage. The pattern penetrated about 2 mm below the surface.

We will now show that a conformal polymer coating is formed in the patterned regions as shown in Scheme 1 and that this coating increases the mechanical stability of the patterns as well as modifying their hydrophobicity. In the following, we will focus mostly on homogeneously exposed monoliths and show that photo-cross-linking yields materials comparable to those obtained with the original technique where cross-linking was induced by thermal dissociation of

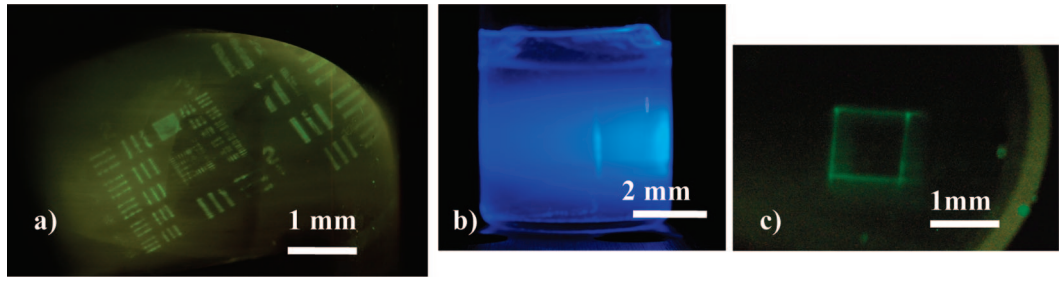

Figure 1. Digital camera images of monoliths photo-cross-linked with 9-vinylanthracene. (a) Surface pattern produced by masking 266 nm light with a standard USAF 1951 resolution calibration mask. (b) Pattern produced by focusing with a 100 mm focal length lens the third harmonic (355 nm) of a pulsed Nd:Yag laser inside a monolith. (c) Pattern produced by focusing 355 nm light inside a gel monolith with a microscope objective. Luminescence was excited in all cases by the 325 nm light of a He−Cd laser. The blue hue in (b) is due to laser glare and to the luminescence of the solvent (acetonitrile) impregnating the wet gel. The solvent of samples (a) and (c) had been exchanged with weakly luminescent methanol, and a high-pass filter was employed to cut the laser glare.

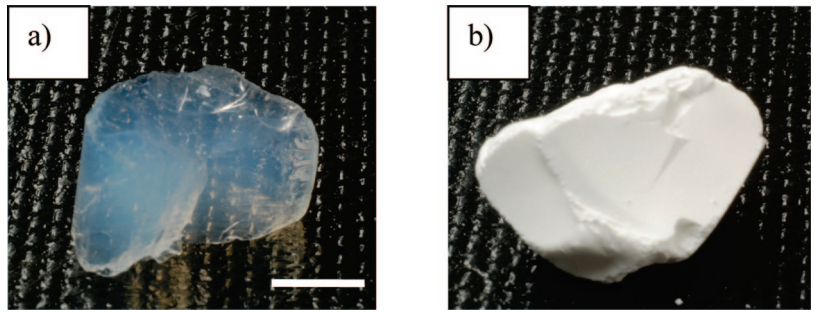

Figure 2. Digital camera image of (a) vinyl-derivatized silica gel monolith after polystyrene photopolymerization and (b) native, nonderivatized monolith. The scale bar represents 3 mm, and both images have the same magnification. The samples contained the same amount of monomer and initiator and were polymerized by exposure to a He−Cd laser expanded by a divergent lens to illuminate the entire sample.

the same initiator AIBN.[17] We will conclude showing that photo-cross-linking allows modulation of physical properties that go beyond the luminescent patterns of Figure 1.

To study the characteristics of photo-cross-linked monoliths we photopolymerized styrene inside native and derivatized monoliths. Silica gels and polystyrene are both transparent in the visible, so the detection of patterns was often difficult. To detect patterns we had to "develop" exposed monoliths, and for this we adapted a strategy that is commonly used for the preparation of polystyrene nano- and microparticles. Polystyrene suspensions are generally prepared by adding an initiator to a styrene solution; to precipitate the polymer, methanol is added to the solution, and a milky precipitate ensues. Thus, after exposure the monoliths were bathed in methanol. Derivatized monoliths exposed to laser light were somewhat hazy after photopolymerization as shown in Figure 2a. Native silica gels photopolymerized under the same illumination conditions became optically opaque as shown in Figure 2b. We reasoned that large, light-scattering polymer particles were formed inside the pores of native silica gels. In derivatized samples polymerization was mostly confined to the pore walls resulting in the formation of smaller particles with minimal scattering.

To confirm the formation of a conformal polymer coating in derivatized gels, native and derivatized samples were analyzed by SEM and AFM. Representative SEM micrographs of monoliths supercritically dried in CO_2 after photopolymerization are shown in Figure 3. Low-magnification images showed relatively flat and homogeneous surfaces for derivatized samples (Figure 3a). Native gels showed small aggregates on their surfaces, consistent with the presence of large polystyrene particles inferred by the optical analysis. High magnification images showed further differences. In silica aerogels, primary silica particles with a diameter in the 2−10 nm range aggregate to form secondary agglomerations with a diameter in the 20−40 nm range. Primary and secondary aggregations were clearly visible in native gels, as shown in parts d and f of Figure 3. In derivatized gels only the secondary aggregations were clearly visible (Figure 3c,e). Overall, the SEM results are consistent with those obtained from samples cross-linked by thermally activated polymerization and indicate that a network of cross-linked silica nanoparticles is formed by photo-cross-linking.

The SEM results were further supported by AFM. Because of the low density of aerogels, the AFM tip tended to lift the samples generating high noise levels. Therefore, xerogels were employed. Figure 4a shows the typical morphology of a vinyl-derivatized sample before photopolymerization. Granular aggregates with a size of tens of nanometers could be resolved, which likely corresponded to the secondary aggregations. After polymerization the size of these aggregations increased (Figure 4b).

Optical, SEM, and AFM analyses show that polymerization of styrene in derivatized gels leads to a conformal coating of the primary silica particles as shown in Scheme 1. In the case of native gels, large, light-scattering polystyrene particles form inside the pores of the matrix but they do not affect the native silica structure. Correspondingly, derivatized monoliths dried supercritically were hydrophobic and floated on water indefinitely. Native samples were very hydrophilic even after photopolymerization and sank immediately. The hydrophobicity of the derivatized, photo-cross-linked samples is very strong evidence of the formation of a conformal coating of the pore walls. If the pore surfaces were not completely coated by the hydrophobic styrene moiety the high hydrophilicity of native silica would cause water to penetrate into the matrix and the monoliths would sink rapidly. High hydrophobicity was also observed in monoliths cross-linked with styrene by thermally activated polymerization, and it represented the best evidence of the formation of a conformal coating.[17]

FT-IR spectroscopy measurements are reported in Figure 5 and provide useful insight on the parameters affecting the cross-linking process. Native monoliths exhibited broad and intense bands below about 1300 cm^{-1} which are characteristic of silica. The most intense of these bands was in the 1100−1200 cm^{-1} range and was attributed to Si−O stretching. In photopolymerized samples (both native and derivatized) we also detected a broad band around 1620 cm^{-1} which was attributed to the breathing modes of the aromatic ring of polystyrene.[21] In samples derivatized with vinyl and methacrylate additional small and narrow bands were detected which most likely were due to the derivatizing moiety. These were at 696 cm^{-1}, which is within the range of CH_2

(21) Ilhan, U. F.; Fabrizio, E. F.; McCorkle, L.; Scheiman, D.; Dass, A.; Palzer, A.; Meador, M. A. B.; Leventis, N. *J. Mater. Chem.* **2006**, *16*, 3046.

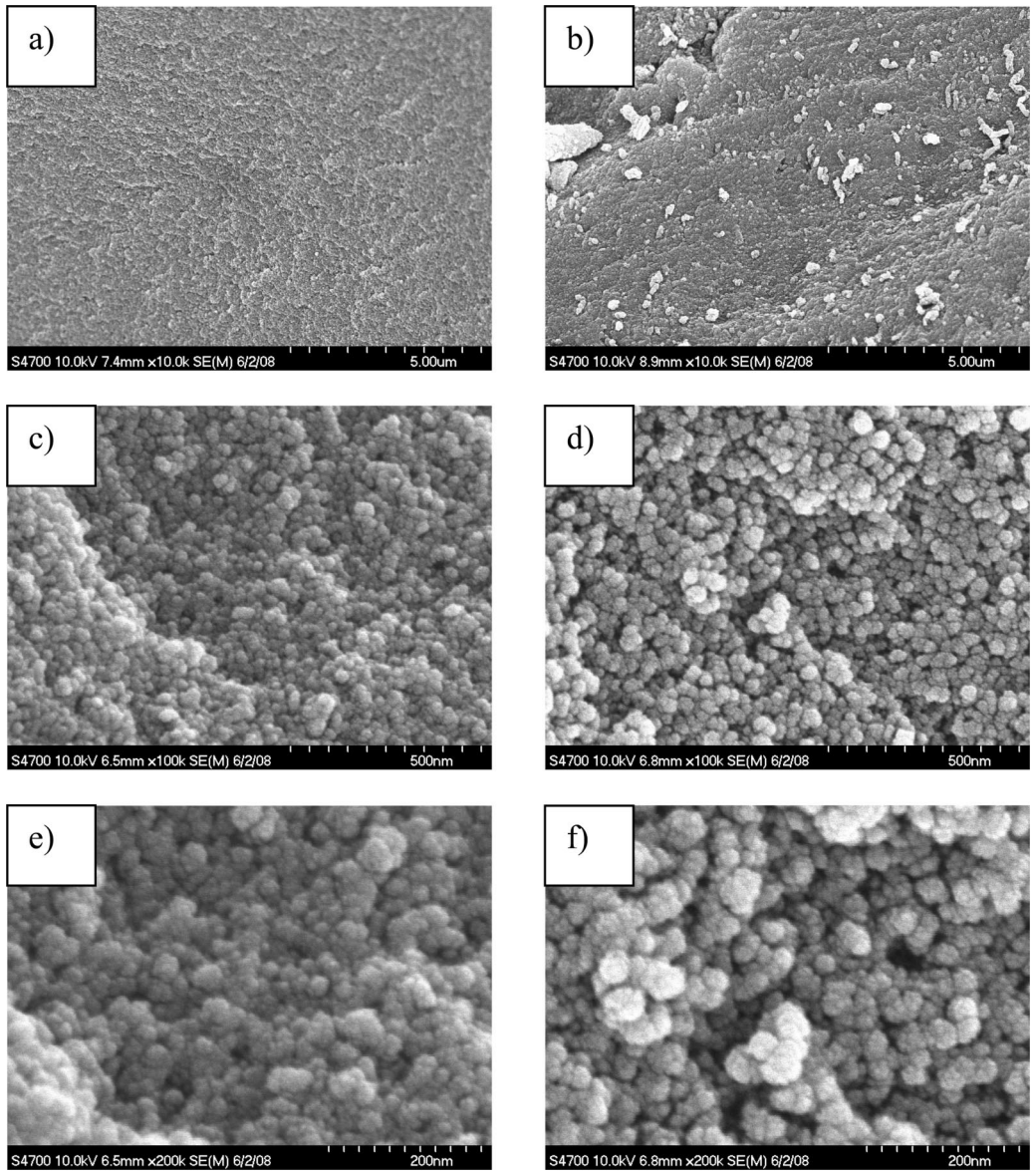

Figure 3. SEM micrographs of silica aerogel monoliths derivatized with vinyl groups during gelation. Left column (a, c, e): monoliths where vinyl groups had been attached to the pore walls during gelation. Right column (b, d, f): native monoliths. Polystyrene had been photopolymerized in all samples before supercritical drying.

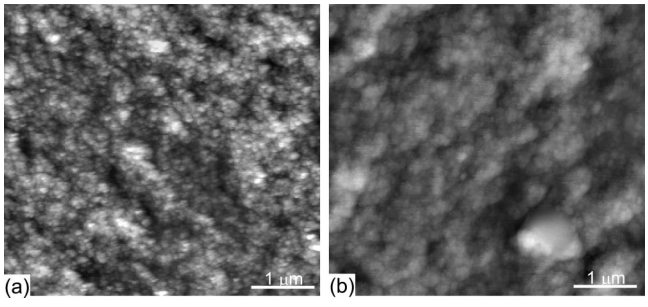

Figure 4. AFM images (5 μm × 5 μm) of vinyl-derivatized silica xerogel (a) before and (b) after photo-cross-linking. The scale bar represents 1 μm.

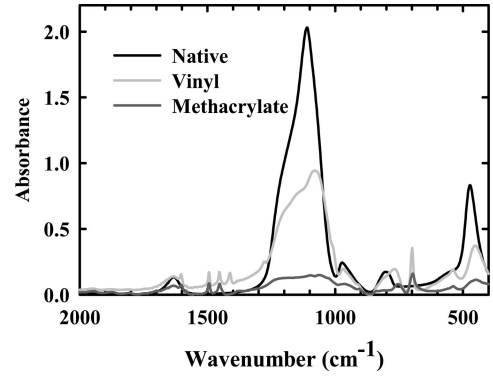

Figure 5. FT-IR spectrum of silica gel monoliths after polystyrene photopolymerization. The derivatization of the pore walls is indicated in the legend.

rocking; at 1409, 1449, and 1493 cm^{-1}, which are within the range of C−H bending, and at 1603 cm^{-1}, which is within the range of C═C stretching. We also noticed that the intensity of the silica bands decreased in derivatized samples. The decrease in the intensity of the silica vibrations is similar to that observed in oxide−polymer core−shell nanoparticles, and it is a further indication that in derivatized

Table 1. Selected Properties of Photo-Cross-Linked Sol−Gel Monoliths

derivatization (light source, irradiation time)	bulk density ($g \cdot cm^{-3}$)	skeletal density ($g \cdot cm^{-3}$)	porosity (%)	surface area [avg pore diameter] ($m^2 \cdot g^{-1}$) [nm]	Young's modulus (MPa)	hardness (GPa)
none (black light, 48 h)	0.243	1.927 ± 0.018	87.3	981 [19.1]	*a*	*a*
vinyl (He−Cd laser, 24 h)	0.215	1.658 ± 0.01	87.0	942 [16.5]	9.63 ± 1.01	2.02 ± 0.01
vinyl (black light, 48 h)	0.418	1.400 ± 0.005	70.1	445 [13.9]	58.79 ± 6.75	8.36 ± 1.63
methacrylate (black light, 24 h)	0.795	1.216 ± 0.002	34.6	55 [24.5]	1000[b]	*b*
methacrylate (black light, 48 h)	0.978	1.043 ± 0.016	6.23	37 [20.1]	1860 ± 130	1.38 ± 0.4

[a] Native gels were very weak, and their mechanical properties could not be tested. [b] Measured with three-point flexural method; hardness not measured.

samples the pore walls are coated with the polymer.[22] The silica bands are reduced by about a factor of 10 in monoliths derivatized with methacrylate, which consistently yielded composites with the highest density and the highest mechanical strength as listed in Table 1. The high cross-linking efficiency of methacrylate is not surprising. In fact, it has been reported before that copolymerization of VTMS with various monomers is inefficient. In the case of styrene, the inefficiency is attributed to the relative stability of the propagating benzyl radicals relative to the higher-energy intermediate that results from addition of propagating benzyl radicals to the surface-confined vinyl.[23] However, in the event where a small amount of vinyl radicals is formed on the surface (by addition of the initiator to dangling vinyl groups), it immediately engages styrene (an energetically exothermic process), leading to cross-linking according to Scheme 1.

Modulating the Physical Properties of Monoliths. The analysis reported above shows that the composites obtained by photo-cross-linking have morphology and physical properties comparable to those of composites obtained by thermally initiated cross-linking. We will now focus on the spatial modulation of the physical properties of bulk monoliths, which is the main advantage of our photo-cross-linking method.

In the early stages of our experiments, we noticed that derivatized monoliths which were exposed to an intense laser source or that contained a high concentration of initiator (e.g., 4% w/w) were nearly transparent; see Figure 2a. Optically dense monoliths were obtained in nonderivatized samples independent of the polymerization rate but also in derivatized samples photopolymerized at a low rate (typically in samples illuminated by a black light). The opacity of nonderivatized samples is likely due to the formation of large, light-scattering particles inside the poors. The different optical properties obtained at different polymerization rates were probably related to the length of the polymer chains in the conformal coating. In samples polymerized at high rates the polymer chains were likely shorter and scattered light less efficiently than those of samples polymerized at low rates. The polymerization rate also affected other physical parameters of photo-cross-linked monoliths such as porosity, density, surface area, and modulus. Table 1 shows that high polymerization rates yielded composites with low density, high porosity, high surface area, and a comparatively small modulus. From Table 1 we also notice that monoliths derivatized with methacrylate and photo-cross-linked at a low rate had the highest modulus. To date, the strongest reported cross-linked materials have been obtained by surface initiated polymerization. The monoliths have a modulus of around 600 MPa, a density of about 0.8 $g \cdot cm^{-3}$, and a porosity of about 38%.[24] Our methacrylate-derivatized samples had a modulus of 1 GPa, a density of about 0.8 $g \cdot cm^{-3}$, and a porosity of about 38%. This result indicates that the slow polymerization rates attainable by photo-cross-linking yield composites with a strength/density ratio higher than those obtained by thermally initiated cross-linking. Exposure time also affected the characteristics of the composites. Long exposures (48 h) yielded composites with a modulus as high as 1.86 GPa, albeit with a comparably high density and low porosity.

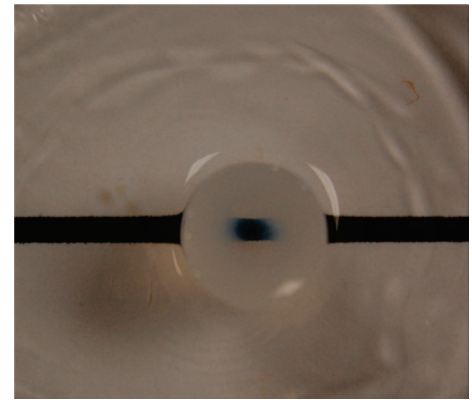

Figure 6. Digital camera image of an optically inhomogeneous wet gel. The sample was a cylinder with a diameter of 7 mm and about 10 mm long. The sample was illuminated with the ultraviolet (325 nm) light from a He−Cd laser. The 3 mm wide beam was incident along the longitudinal direction and passed through the center of the cylinder. The sample was placed on a Petri dish, and it was photographed from the top against a background of a white sheet of paper with a black line running across. The central part of the monolith is transparent because the high intensity of the incident light induced high polymerization rates, which in turn generated short, nonscattering polymer strands. The periphery of the monolith was illuminated by scattered light, and the lower polymerization rate leads to larger, light scattering polymer aggregates.

Optical properties of monoliths could also be varied by varying the illumination conditions. For example, optically inhomogeneous monoliths could be fabricated as shown in Figure 6. The central region of the monolith was illuminated with a low-divergence laser beam incident along the axis of the cylindrical monoliths. In the center of the monolith, the light had the highest intensity. The polymerization rate was high, and small polymer particles formed which did not

(22) Lin-Vien, D.; Colthup, N. B.; Fateley, W. G.; Graselli, J. G. *The Handbook of Infrared and Raman Characteristic Frequencies of Organic Molecules*; Academic Press: Boston, 1991.
(23) Liu, P. *Colloids Surf., A* **2006**, *291*, 155.
(24) Gatic, N.; Fernandez, N.; Opazo, A.; Alegria, S.; Gargallo, L.; Radic, D. *Polym. Int.* **2003**, *52*, 1280.
(25) Mulik, S.; Sotiriou-Leventis, C.; Churu, G.; Lu, H.; Leventis, N. *Chem. Mater.* **2008**, *20*, 5035.
(26) Lu, H.; Wang, B.; Ma, J.; Huang, G.; Viswanathan, H. *Mech. Time-Depend. Mater.* **2003**, *7*, 189.

scatter light very efficiently. The outer regions were illuminated by stray light, resulting in a lower polymerization rate and in the formation of large, light-scattering polymer aggregates. Figure 6 complements therefore the results of Figure 1 and demonstrates that physical properties such as optical absorption, emission, hydrophobicity, and mechanical strength can be tuned within a same monolith by photopolymerization.

In conclusion, we have shown that bulk sol−gel monoliths with spatially modulated physical properties can be produced by photo-cross-linking. Surface and three-dimensional patterns are obtained by using suitable light sources and illumination conditions. Our method is simple and extremely versatile, since it combines the flexibility of sol−gel and polymer chemistry. Multifunctional sol−gel monoliths can now be realized which have potential applications in microfluidics, optics, mechanics, and acoustics.

Acknowledgment. Leventis and Lu acknowledge the support of NSF under CMMI-0653919 and CMMI-0653970. We thank Fang Wang for conducting nanoindentation measurements.

CM803374B

(27) Oliver, W. C.; Pharr, G. M. *J. Mater. Res.* **1992**, *7*, 1564.